California Polytechnic
State University

Time Variation of the Broad Hβ and Hα Emission Lines in Active Galactic Nuclei

A Senior Project
Presented to the Department of Physics

Author:
Bryan R. Scott

Advisor:
Dr. Vardha N. Bennert

Title Page: SDSS DR6 Optical Images for the Eight Objects studied in this paper.
Above: Sunset over Lick Observatory during follow-up observations in January 2013.

Date of Last Revision: December 16, 2013

Abstract

High-quality Keck/LRIS long-slit spectra for a sample of 97 active galaxies selected from the Sloan Digital Sky Survey ($0.02 \geqslant z \geqslant 0.1$; MBH $\geqslant 10^7$ $M_\odot$) were obtained between January 2009 and March 2010 in order to study the black hole (BH) mass scaling relation in the local universe. Typically, the width of the broad Hβ emission line is used to measure the mass of the black hole (M_{BH}). However, signs of variability in the emission line profile are seen for eight objects: While broad Hβ emission lines had previously been observed in spectra from the Sloan Digital Sky Survey (SDSS), they are missing in the Keck spectra. Based on seeing and PSF profile arguments, we can exclude that the lack of broad lines in the Keck spectra are caused by the telescope being pointed off center, missing the active nucleus. Follow-up observations were conducted in January and March 2013 in both Hβ, as well as Hα (which had not been obtained at Keck) using the Kast spectrograph mounted on the Shane three meter telescope at Lick observatory. Since SDSS uses a 3 arcsec fiber, the position angle of these long-slit observations was set perpendicular to the angle of the Keck longslit observations in order to search for any off-center broad emission. The broad emission lines remain missing in Hβ and are missing or reduced in Hα, suggesting changes in Seyfert classification transitions on timescales of approximately a decade. Observational constraints make variability of the torus or broad-line region over time as the most likely cause for this variation. However, at least in some cases, the existence of an AGN that is non-coincident with the center of the host galaxy due to an ongoing merger or gravitational recoil cannot be ruled out. The most promising candidate for such a scenario is SDSS J10383+4658 which shows a blue knot just off-center from the host galaxy, and could have been missed in Keck observations but is included in the SDSS fiber.

Contents

List of Figures

List of Tables

1 Introduction

Active Galactic Nuclei (AGN) are a highly energetic phenomenon observed in the central regions of galaxies which cannot by otherwise attributed to stellar activity. The earliest evidence of the existence of these objects is credited to Carl Seyfert, who published a paper in 1943 in which he identified 12 galaxies which had unique spectral characteristics. These objects would come to be called Seyfert galaxies, and are distinguished by the visibility of the host galaxy.

Among other interesting features, these galaxies have broad high ionization emission lines whose source was unknown. Optical images of these galaxies revealed that they contained bright regions, with star like emission characteristics, in their central regions. While there remains some ambiguity in the definition of what constitutes the large number of AGN subtypes, this quality has given rise to the name Quasi-Stellar Object, or Quasar in the vernacular. Further surveys have led to the discovery of radio active galaxies, Blazars, and Low Ionization Nuclear Emission Region Galaxies (LINERS) among others. Additionally, AGNs are subdivided into type categorizations depending on the degree to which their spectra show broad emission lines. The unified model of AGN structure has provided a model by which the large number of subtypes of AGN can be explained. Despite this, there is some suspicion that the AGN type classification (§ 1.4) may not be fixed, and it is this question that this paper will address.

1.1 AGN Mechanism

Although Active Galaxies were identified as unique objects by the mid-1940s, the mechanism underlying AGN emission was not well understood until much later. Any possible explanation was constrained by a number of key observations. The first, was that Active Galaxies are extremely luminous, on the order of 10^{11} $L_{\odot}$, and the second was that light travel time arguments constrained the central engine of an Active Galaxy to a small region, on the order of light days across. Unless otherwise stated, the references for the following sections are *An Introduction to Active Galactic Nuclei* and *Supermassive Black Holes in Galactic Nuclei: Past, Present and Future Research.* [1] [2]

The lifetime of an AGN places constraints on their nature according to a simple argument based on two observations. First, large surveys of AGN estimate that $\approx 1\%$ of galaxies are currently classified as active, and second, the age of the universe is on the order of 10^{10} years. If all AGN are always active, than their lifespan is therefore roughly equivalent to the age of the universe, or about 10^{10} years. On the other hand, if galaxies pass through an active phase, which is more likely and observationally supported, than AGN lifespan is approximately 1% of 10^{10} or 10^{8} years. In either case, AGNs are comparatively long lived given their luminosity, and they must be very massive in order to sustain mass to energy conversion.

If the assumption is made that the central AGN source is stable and isotropic, a mass estimate can be derived from AGN luminosity. For stability, the inward gravitational force and the outward radiation force must be balanced.

$$\frac{\sigma_e L}{4\pi c r^2} \leqslant \frac{GMm_p}{r^2} \tag{1}$$

Where σ_e is the interaction cross section of the electron, L is the luminosity of the AGN, c is the speed of light, r is the distance, M is the mass of the AGN, with m_e and m_p being the mass of the electron and proton respectively. It is important to note that this arises because radiation pressure primarily acts on electrons, while gravity primarily acts on protons. Solving for the luminosity,

$$L \leqslant \frac{4\pi G c m_p}{\sigma_e} M \tag{2}$$

AGN flux varies on timescales of days, and flares can occur on even shorter time scales. This restricts the physical size of the AGN central engine to a region comparable to the light travel time. With high luminosity and small size, the process of mass to energy conversion which drives emission must be very efficient. Mass to energy conversion is given by the equation:

$$E = \eta m c^2 \tag{3}$$

Here, η is the efficiency of the energy conversion process. Correspondingly, the rate at which energy is extracted via a process is given by:

$$L = \eta \dot{M} c^2 \tag{4}$$

Assuming the energy conversion process is accretion, the rate of accretion $\dot{M}$ is consequently given by:

$$\dot{M} = \frac{L}{\eta c^2} \tag{5}$$

In order to determine if accretion is a viable mechanism for sustaining mass to energy conversion in AGN, an estimate of η is required. The rate at which gravitational potential energy can be converted is given by:

$$L \approx \frac{dU}{dt} = \frac{GM}{r}\frac{dm}{dt} = \frac{GM\dot{M}}{r} \tag{6}$$

By comparison:

$$\eta \propto \frac{M}{r} \tag{7}$$

With a mass estimate of 10^8 solar masses, an estimate of the radius of the AGN central engine will yield an estimate of the η parameter. This can be determined if we make the limiting case assumption that the system is maximally compact, i.e. a black hole. The radius of a non-rotating black hole is called the Schwarzschild radius, and is given by:

$$R_s = \frac{2GM}{c^2} \tag{8}$$

Substituting into equation 7, we find that $\eta \approx 0.1$, which is more efficient than hydrogen to helium fusion ($\eta \approx 0.007$) which constrains any model of the AGN central engine and calls into question the idea that AGN activity is attributable to, for instance,

an extremely dense stellar cluster. Coupled with additional observational evidence, discussed in the following sections, and given the large known mass of AGN central engines, the scientific consensus is that AGN emission is the result of accretion onto a black hole with a mass on the order of 10^9 $M_\odot$ or larger. These objects have come to be called "supermassive" in order to distinguish them from smaller stellar mass black holes.

1.2 Spectral Features

1.2.1 Narrow and Broad Emission Lines

A key feature which distinguished AGNs early on and remains of scientific interest is the presence of broad emission lines in spectra which are believed to result from Doppler broadening. Doppler broadening occurs when atoms emitting photons are at different velocities relative to an observer. Gas traveling in the potential of a black hole will have a different velocity relative to an observer depending on the point at which it is in its orbit. With a different velocity, it will have a different redshift (or blueshift) for an observer. The integrated effect of this is to produce broad emission lines.

These broad emission lines can have a considerable amount of variation in strength and profile among different lines, which offers some evidence for suspecting that the broad line region is not homogeneous. The region responsible for this emission is commonly referred to as the Broad Line Region (BLR). Additionally, the integrated flux in the broad lines can vary considerably over time in a way that is correlated with changes in the continuum emission. This is one reason why it is believed that the BLR is photoionized by the central engine.

Another feature of AGN spectra are a series of narrow emission lines. It is believed that low densities in the narrow line region as compared to the broad line region prevents transitions from being collisionally suppressed. Forbidden transitions, which can occur if electrons are raised to an excited state, have transitions which are typically forbidden along the electric dipole path by quantum mechanical selection rules and do not occur at high frequencies in the broad line regions due to the higher density of this region. These transitions occur more frequently in the narrow line region (NLR), leading to prominent narrow emission lines.

Dust in these regions, however, complicates spectral analysis. While forbidden line transitions occur isotropically, the spatial extent of dust in these regions can cause orientation effects to be present in the narrow line and broad lines. Like the BLR, flux ratios between emission lines suggest that the NLR is photoionized by the AGN continuum, and not stars in the nuclear region. Figure 1 is a typical type 1 AGN spectra showing clear broad and narrow emission lines.

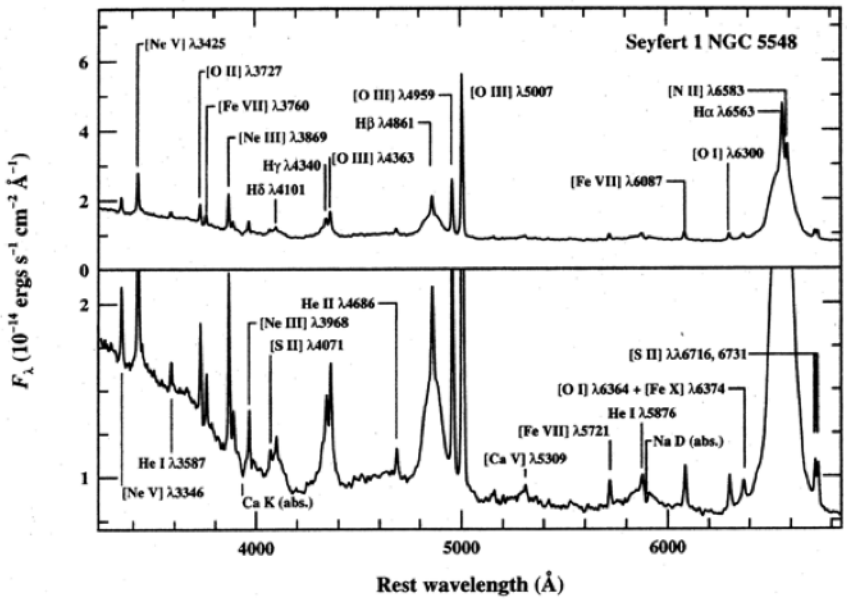

Figure 1: Spectra of the type 1 Seyfert NGC 5548 showing clear broad and narrow emission line components. These broad emission lines distinguish type 1 AGN from type 2 AGN.

1.2.2 Continuum

In addition to the broad and narrow emission lines, another feature of AGN spectra is the underlying featureless continuum. The name refers to the lack of clear absorption and emission lines. The continuum is distinguished from a more typical stellar blackbody distribution by a pronounced power law. The continuum is believed to be produced by both thermal (i.e. due to particles with a Maxwellian distribution) and non-thermal (particles producing synchrotron radiation) emission. The scientific consensus is that continuum emission arises from gas in the accretion disk.

1.3 AGN Structure and Measurement of SMBH Mass

Taken together, this paints a compelling picture of the structure of these objects. AGNs consist of a central BH surrounded by an obscuring torus. The BLR, which consists of ionized clouds, is largely enclosed within the torus. The region responsible for the narrow emission lines is largely outside this torus. Since changes in the AGN continuum proceed changes in the broad line region, it is clear that the AGN and the BLR are not spatially coincident.

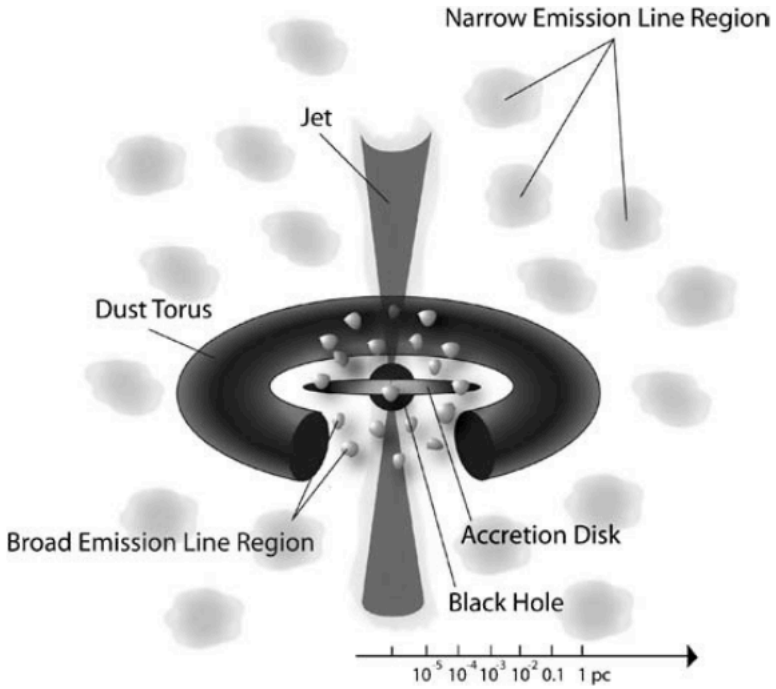

Figure 2: Diagram of AGN structure. The central engine is surrounded by an accretion disk, the BLR and a dusty torus. Outside this torus is the NLR. [2]

The proximity of the BLR to the central engine of the AGN proves to be a powerful tool for measuring the mass of the central engine. Since the broad line region varies in flux over time scales of light-days to weeks, while the continuum source varies on shorter time scales, the lag in flux variability of the line emitting regions can be used to measure the size of the BLR. This technique has come to be called reverberation mapping. The virial theorem, coupled with assumptions about the geometry of AGNs, and the velocity of the line emitting gas (e.g. the velocity of the clouds in the BLR) provides the following simple formula for black hole mass. M_{BH} can be determined by exploiting Doppler broadening. Gas in the broad line region is in the potential of the black hole, and at each point has a different velocity relative to an observer. The result is that the gas is differentially redshifted and blueshifted to an observer, and becomes broad. The width of this line gives the velocity of the gas, and combined with distance measurements, can be used to determine the mass of the black hole via equation 9.

$$M = \frac{fr\sigma^2}{G} \tag{9}$$

Here velocity, denoted by σ, is given by the width of the broad spectral line at half the peak of the line, while the distance r is determined via reverberation mapping. The parameter, f is known as the "fudge factor" and incorporates assumptions about the geometry of the central regions of the AGN. Estimates of f can be made by matching scaling relations (§ 1.5) for inactive and active galaxies.

Type	Criteria
Type 1	Broad and Narrow Emission Lines
Type 2	Narrow Emission Lines Only
Type 1.5	Both Components can be Easily Identified
Type 1.8	Weak but visible in Hβ and Hα
Type 1.9	Not visible in Hβ but weak in Hα

Table 1: The expanded AGN type classification scheme based on the relative strengths of the Hβ and Hα emission lines.

1.4 Unification

The wide variety of AGN types has challenged explanation. Why are some objects highly luminous, while others less so? Why do some objects have both broad and narrow lines, while others only have narrow lines? Are these differences a result of intrinsic differences in the structure of these objects, or is there some other explanation? While orientation was recognized as being important to the understanding of these objects early on, it is now believed that varying orientation relative to the line of sight is responsible for the observational differences in AGN.

Indeed, the model of AGN structure suggests the unification scheme for active galactic nuclei. Rather than several distinct types of objects, all AGN represent similar phenomena. It is believed that there is no fundamental difference between the observed types of AGNs, rather, it is thought that differences in spectra and luminosity arise primarily from their orientation relative to an observer. The simplest unification schemes hold that there are two basic spectroscopic classifications of AGN, type 1 and type 2. Type 1 AGN have both narrow and broad lines, while type 2 AGN only have the narrow lines. Additionally, spectra can be further classified as type 1.5, 1.8 and 1.9 based primarily on the relative strengths of Balmer emission lines, though He I and He II emission lines are sometimes included as well. [3] Table 1 summarizes the type classifications.

Type 1 AGN have prominent broad and narrow Balmer emission lines, while type 2 AGN lack broad emission lines. Type 1.5 AGN have clearly identifiable broad and narrow emission lines, and are particularly characterized by a narrow component which appears to be superimposed upon an underlying broad component. Type 1.8 nuclei have very weak but identifiable broad Hβ and Hα emission lines, while type 1.9 lack the broad component in Hβ and retain it in Hα.

The AGN unification scheme proposes that what determines classification between type 1 and 2 is the viewing angle through which the object is observed at.

As before, it is thought that the central regions of AGN consist of a SMBH surrounded by an accretion disk and the broad line region. This is enclosed by a dusty torus which obscures the BLR depending on the orientation of an observer. This accounts for the lack of broad lines in type 2 AGN. The NLR is outside the torus, and thus remains unobscured independent of viewing angle. Emission from the SMBH and accretion disk can escape only along the axis of the torus, which prohibits the isotropic emission of radiation from the SMBH. This means that an observer viewing the AGN

face on will observe both narrow and broad emission lines in spectra. The following figure illustrates this.

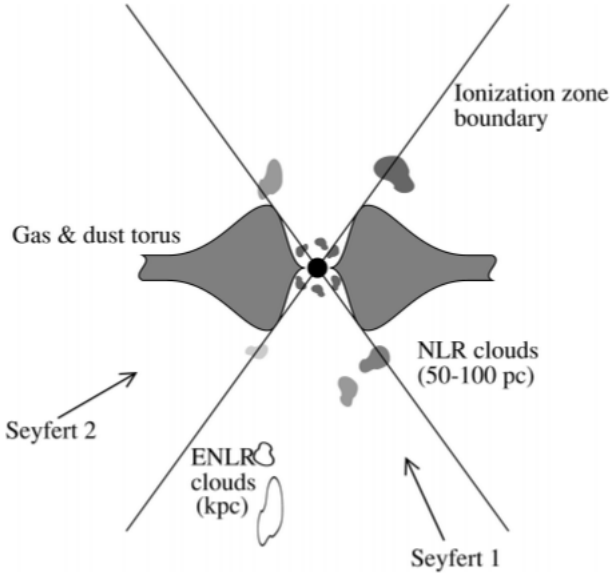

Figure 3: Diagram demonstrating models of AGN unification. The angle with which an observer views an AGN determines its type classification. Viewers who see the AGN edge on see an obscured AGN and classify it as a type 2, while viewers who observe the AGN face on see an unobscured type 1. [1]

An important test of this model would be to detect broad lines in the polarized spectra of type 2 AGN. Light from the broad line region is emitted isotropically and can scatter off electrons in the NLR towards an observer who is otherwise unable to observer the broad line region. When this occurs, the light becomes polarized. If the unification picture is correct, it should be possible to detect broad lines in polarized spectra from a Type 2 AGN. This was first accomplished by looking at polarized light from the galaxy NGC 1068 and has since been accomplished for dozens of other objects. [1]

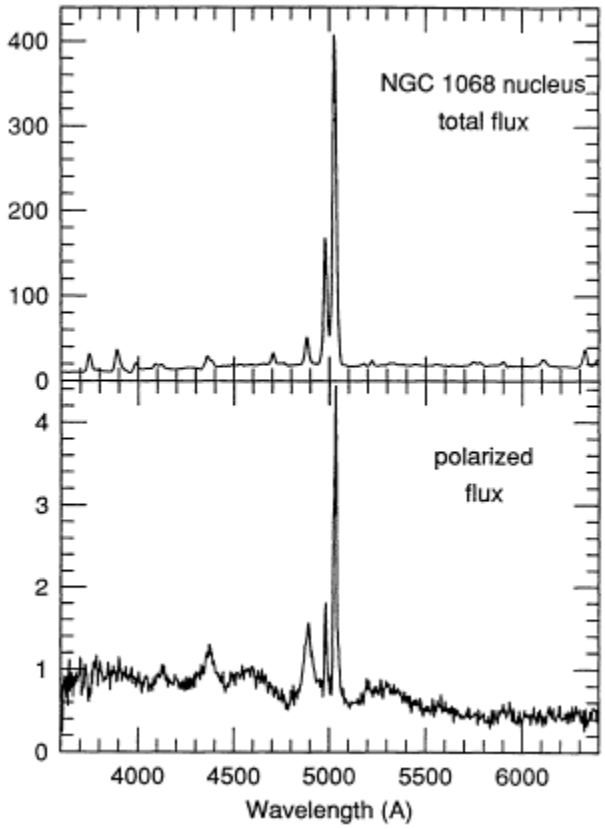

Figure 4: Spectra from NGC 1068 showing typical Seyfert 2 flux, with a typical Seyfert 1 spectra in polarized(i.e. reflected) flux. [1]

While this model provides a powerful starting point for understanding differences in AGN classification, it remains likely that other parameters impact classification. AGN are likely to have different gas and dust content and there may be differences in the geometries of the dusty torus, which surround the BLR, or in the structure of the BLR itself. Under one such scenario, dust and gas initially obscures the central regions, producing a type 2 AGN, while at a later time the gas and dust blows free, leading to the appearance of a type 1 (§ 4.3).

1.5 Black Hole Mass Scaling Relations and Formation Models

The discovery of a relation between the mass of the SMBH and the stellar velocity dispersion σ, a measure of how stars are moving in the central regions of a galaxy, and hence the mass of the host galaxy has been interpreted as linking the formation of SMBHs to the formation of their host galaxies. Additional relationships have been found between SMBH mass and host galaxy luminosity (M-L relation) and bulge mass (M-M_{Bulge} relation). These relationships are unexpected, given that the mass of the

SMBH is as much as three orders of magnitude smaller than the mass of their host galaxy. The current best measurement of the M-σ relation comes from a fit to the observations recorded in figure 5.

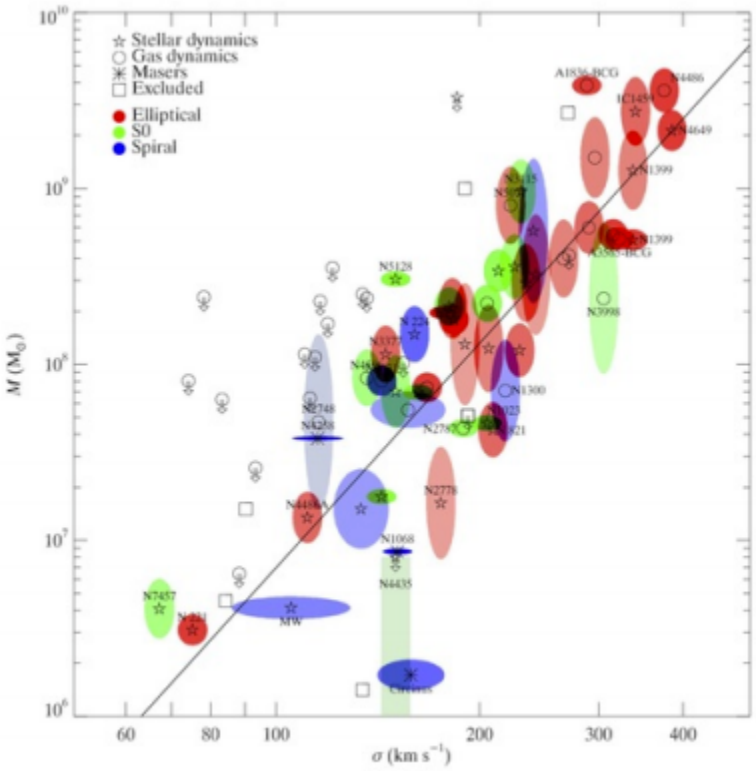

Figure 5: The most recent measure of the M-σ relation. Different sources are distinguished by color and marker shape, which indicated measurement method. [6]

The formation of SMBHs remains an open question with three competing models. (Volonteri, 2012) These models are summarized in Figure 6.

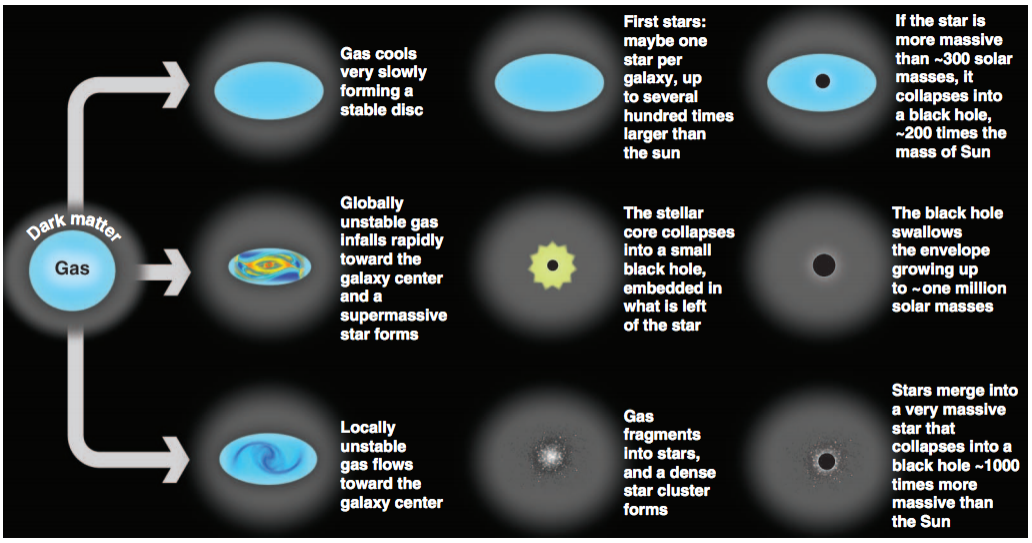

Figure 6: Diagram of three SMBH formation models. Each scenario is constrained by its ability to reproduce the various scaling relations. [7]

Each scenario begins with early galaxy seeds, consisting of a condensed gas at the center of dark matter halos. From there, the seeds of todays large black holes follow one of three paths. Under the first scenario, SMBH are formed from the remnants of Population III stars. These first generation stars collapse into smaller seed black holes, which grow through mergers into the large black holes we see today. Under the second scenario, large stars can form due to instabilities in proto-galaxies. These supermassive stars are rotationally supported until under going collapse due to gravitational instability, directly producing black holes on the order of 10^6 $M_\odot$. The final scenario involves gas being driven to the central regions of early galaxies, where star formation occurs. The high density of stars in this region leads to mergers and black hole formation, producing seed black holes with masses of around 10^3 $M_\odot$.

A key observational test of black hole and galaxy formation models is their ability to reproduce the various scaling relationships. The primary goal of this ongoing study is to better quantify the M-σ relation according to slope and scatter for galaxies in the local universe. [4] [5] However, challenges to measurement of the width of the broad Hβ emission line provided evidence of time variability of the emission lines used to constrain this relation.

2 Goal of Thesis

In conducting fitting of the broad lines to measure the mass of SMBH in a sample of 97 local AGN, 8 objects were found to be missing clearly identifiable broad emission lines in Hβ, lines which had previously been observed to be present. Followup observations revealed similar changes in the appearance of the Hα lines. The goal of this paper is determine whether the variability in the Hα and Hβ emission lines is due to a physical

process, and if so, to understand the source of the variability. Following this, it is the goal to place constraints on and to classify this variability using follow-up observations and to understand the effect of telescope pointing and seeing on Keck observations. Lastly, potential mechanisms should be understood, and observational signatures for each mechanism constrained.

3 Sample Selection, Observations and Data Reduction

Type 1 AGNs were selected from Sloan Digital Sky Survey (SDSS) Data Release 6 for black hole mass estimates $\geqslant 10^7 M_\odot$ from continuum luminosity and full width at half max of the broad Hβ emission line. The Sloan Digital Sky Survey uses a fiber with a 3" diameter on a 2.8 meter ground based telescope. Sloan data comes reduced from the SDSS archive, and images and spectra are taken from the SDSS Data Release 6.

Objects were visually inspected to ensure no misclassification and additional observations were taken of 97 objects between January 2009 and March 2010 with the Low Resolution Imaging Spectrometer (LRIS) at Keck I. Data Reduction for Keck was conducted by Vardha N. Bennert and includes the standard reduction steps such as bias subtraction, flat fielding, and cosmic ray rejection. Arc-lamps were used for wavelength calibration in the blue spectral range, sky emission lines in the red. A0V Hipparcos stars, observed immediately after a group of objects close in coordinates were used to correct for telluric absorption and perform relative flux calibration. [4] [5]

From these final reduced 2D spectra, 1D spectra were extracted. A central spectrum with a width of 1.08 arcsec (8 pixels) was extracted to measure the Hβ width for BH mass determination, that is, encompassing the broad-line region (BLR) emission given a typical seeing of 1 arcsec and a slit width of 1 arcsec. The slit was oriented along the major axis of the host galaxy.

Follow-up observations were conducted for 8 objects in January and March 2013 at Lick Observatory using the Kast spectrograph mounted on the Shane 3 meter telescope with a 2 arcsec slit width. Data reduction for Lick observations was conducted by William Keel and included standard reduction steps. Arc-lamps were used for wavelength calibration. The slit was oriented either along the major axis of the galaxy or perpendicular to the Keck slit orientation, as in figures 10 and 11.

From these 2D spectra, 1D spectra were extracted with a 4 pixel ($\approx$ 3") width to mimic the Sloan fiber's 3" diameter, and was centered on the peak in flux.

Object #	RA+DEC	Redshift	Keck Date	Lick Date	SDSS Date
8	08 47 48.28 +18 24 39.9	0.085	2009 Jan 22	2013 Jan 15	2005 Dec 7
27	09 32 59.60 +04 05 06.0	0.059	2010 Jan 14	2013 Mar 11	2001 Dec 21
28	09 38 12.27 +07 43 40.0	0.0218	2010 Jan 14	2013 Jan 15	2003 Apr 4
157	10 38 33.42 +46 58 06.6	0.0631	2010 Jan 14	2013 Jan 17	2002 Dec 12
209	14 23 38.43 +27 20 09.7	0.0639	2010 Mar 14	2013 Mar 12	2006 May 26
207	13 53 45.93 +39 51 01.6	0.0626	2010 Mar 14	2013 Mar 12	2004 Feb 26
38	11 18 53.02 +28 27 57.6	0.0599	2010 Jan 15	2013 Mar 11	2006 Feb 27
40	11 40 54.09 +23 07 44.4	0.0348	2010 Jan 15	2013 Jan 13	2006 May 21

Table 2: The objects which appear to exhibit variation in the broad emission lines (§4.3) are given with the Right ascension and declination, redshift and the date of observation by SDSS and at Keck and Lick Observatories.

Keck observations were carried out on 2009 January 22 (clear, seeing $\approx$ 1. 1), 2009 2010 January 14 (clear, seeing $\approx$ 1. 2), 2010 January 15 (low clouds, seeing $\approx$ 1), 2010 March 14 (scattered clouds, seeing $\approx$ 0. 8"). § 4.5 contains a discussion of the effect of seeing on Keck observations. Conditions at Lick observatory during observations were clear with minimal scattered clouds.

4 Analysis

4.1 Stellar Subtraction

After standard data reduction steps, the contribution of stars in the host galaxies was accounted for using a script written for the purpose of stellar absorption spectra subtraction. This script fit a linear combination of known stellar profiles, according to the age of the stellar population in the host galaxy, to the Keck and SDSS spectra, and allowed for the isolation of the AGN spectra from that of these stars. Masking the broad emission lines allows for an accurate fit of the stellar continuum.

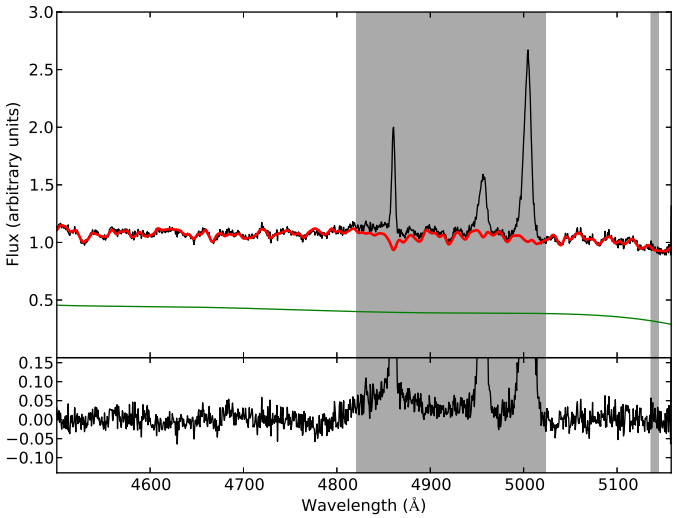

Figure 7: Example of stellar subtraction fit window. The red curve is the fit to stellar absorption lines in the host galaxy.

A poor signal to noise ratio in Lick spectra prevented fitting of a stellar absorption profile to the spectra. However any absorption lines present in Lick spectra is likely to be negligible compared to flux from continuum source.

4.2 Fitting of Emission Lines

The Hβ broad emission line, as well as the nearby [O III] narrow emission lines were fit using a script written by Matthew Auger. This script fits a polynomial (specifically, Hermitian) fit of a given order for the broad and narrow Hβ components, as well as the [O III] lines.

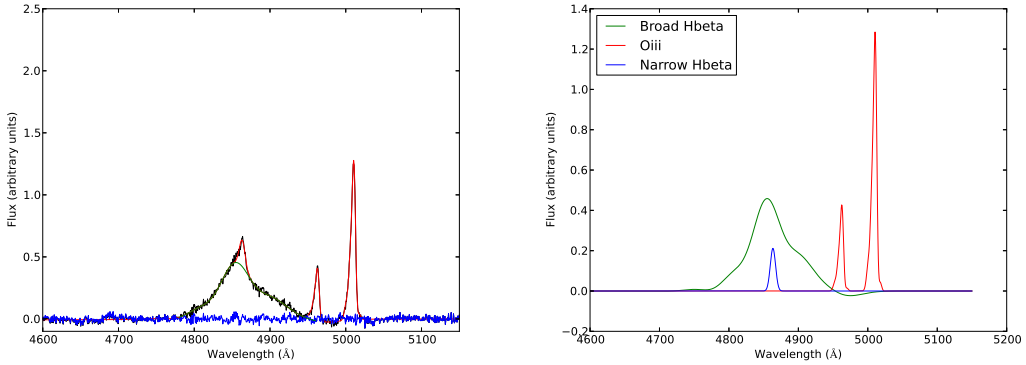

Figure 8: Left Panel: Example composite fit to the data. Right Panel: Example component fit in the region around Hβ for L71, an object not discussed in this paper, which has a clear broad component fit. The narrow [O III] and broad Hβ emission lines are fit with a Hermitian polynomial.

Similarly, the Hα emission line and surrounding lines are fit using a more complex set of polynomials and gaussians.

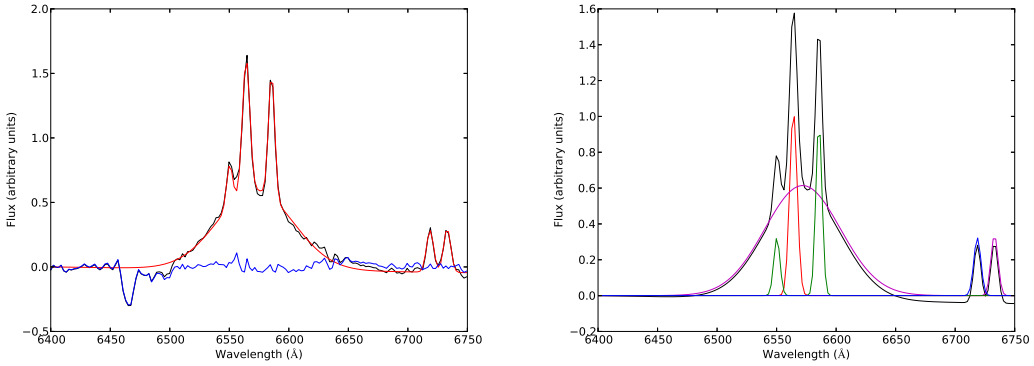

Figure 9: Left Panel: Example composite fit to the data. Right Panel: Example component fit in the region around Hα for L157, an object which exhibits signs of emission line variability, as discussed in the following sections. Narrow Hα is fit with a Gaussian, Broad Hα with a Gauss-Hermite polynomial, narrow NII with a Gaussian and the continuum is fit with a first order polynomial.

As outlined above, the FWHM of the Hβ broad component is taken in order to estimate the mass of the SMBH, however for a subset of the 97 objects in the survey, eight objects lacked a distinct broad line. It is these objects that we study for signs of emission line variability.

4.3 Emission Line Variabiltiy

4.3.1 Hβ Emission Line Variability

Eight of 97 objects in the survey showed signs of variability between the Sloan and Keck observations. These objects show substantial broadening of the Hβ emission line in SDSS spectra, while showing much reduced broad emission in Keck spectra. Though of significantly lower quality, Lick observations do not show signs of $H\beta$ broad emission for any of the objects in the sample. Figures 10 and 11 illustrate the progression of broad emission for the sample.

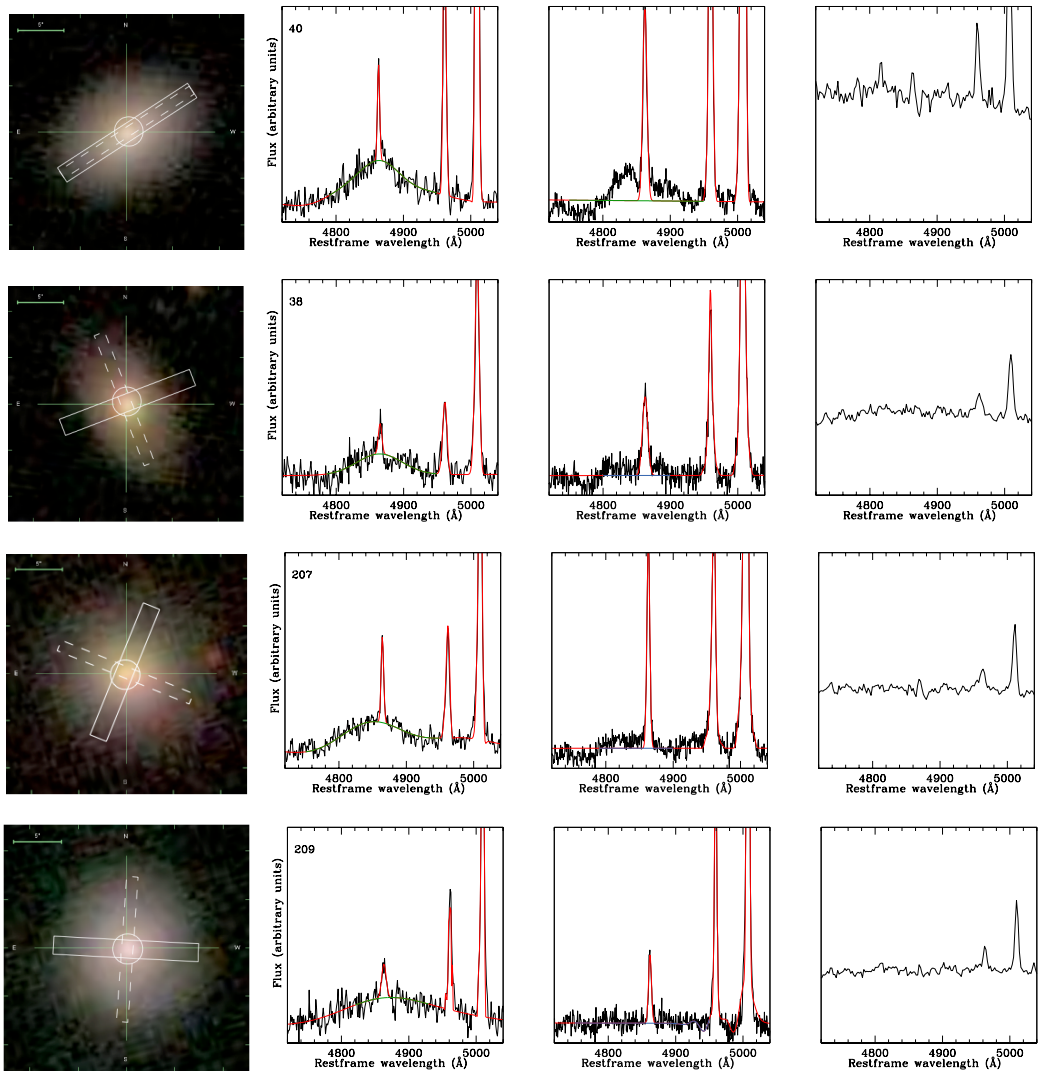

Figure 10: Left column, SDSS optical image for objects 40, 38, 207 and 209 from top to bottom. The SDSS image of each galaxy is overlaid with the slit position for Lick (solid box) and Keck (dashed box), and the SDSS fiber (solid circle) is positioned on the centering target of the host galaxy. In the other columns, the SDSS, Keck and Lick spectra are shown, with the red line being the spectra, green line representing either the Hβ fit region (Keck) or the fit to the broad line (SDSS). Due to the low signal to noise ratio, no fit is done for Lick spectra.

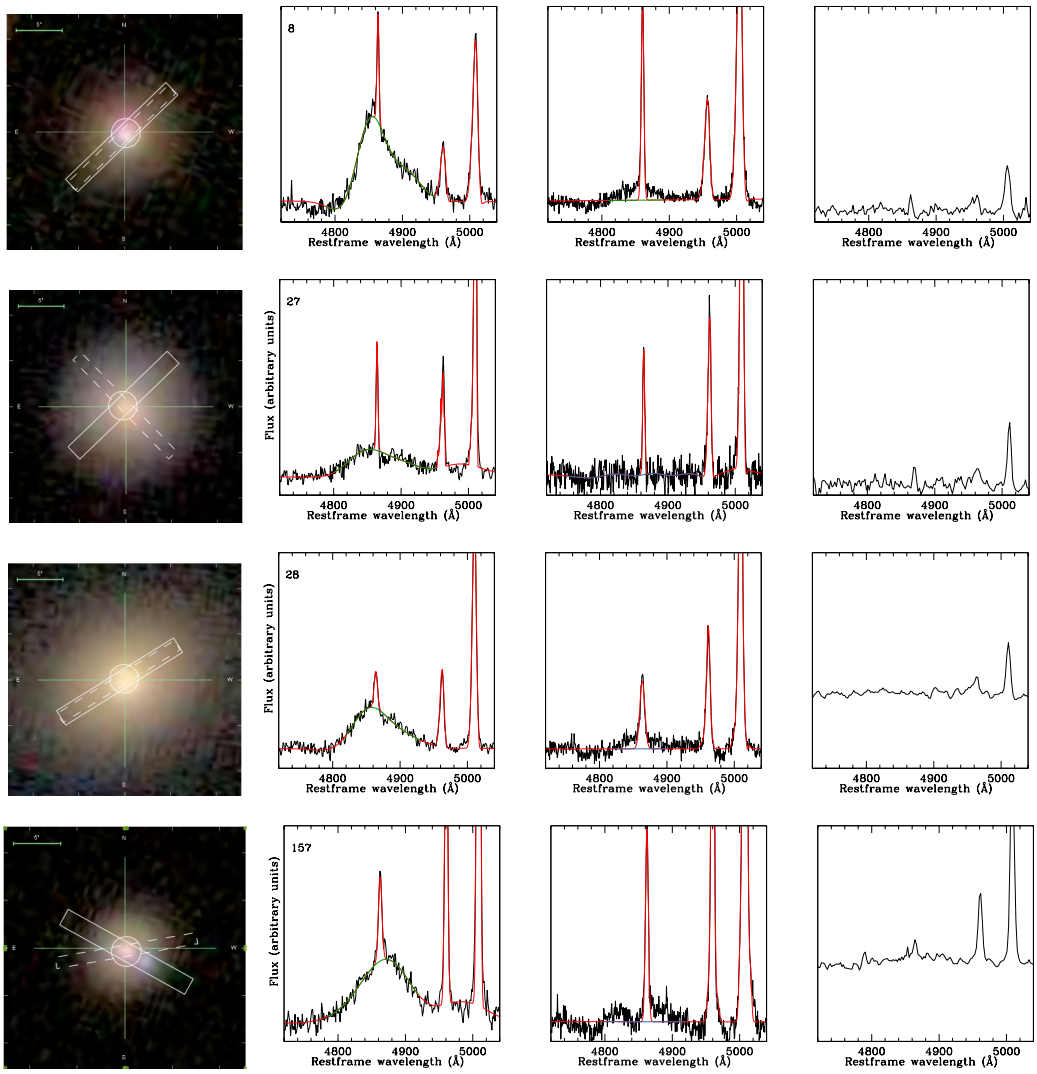

Figure 11: Same as in Figure 10 for objects 8, 27, 28 and 157 from top to bottom.

Each object in figures 10 and 11 show a lack of, or significantly reduced, broad Hβ emission between Sloan spectra and later Keck spectra.

4.3.2 Hα Emission Line Variability

Since variability in Hβ for the eight objects precluded the use of this line to measure the mass of the AGN central engine, an attempt was made to make Hermitian polynomial fits of another Balmer line, Hα using SDSS spectra. Hermitian polynomials are commonly used in emission line fitting to account for line asymmetries. In SDSS,

these emission lines show significant Doppler broadening. Follow-up Lick spectra, however, shows reduced broadening of the Hα emission line for six of the eight objects. Keck spectra do not cover the region containing Hα. Figures 12 and 13 illustrate the progression of the Hα emission line between SDSS spectra and Lick spectra.

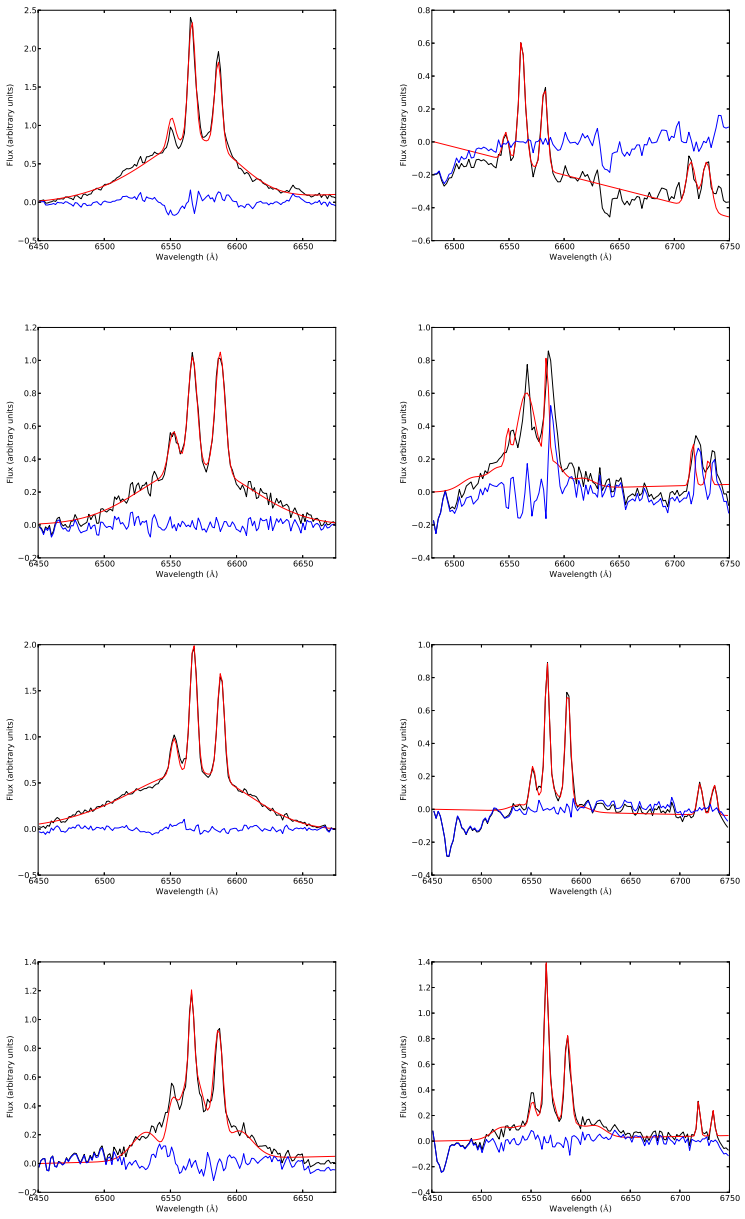

Figure 12: SDSS (left) and Lick (right) spectra in Hα for objects 40, 38, 207, 209 with composite fit(red) to the emission lines. The broad component underlying the emission lines in this region is due to broadening of the Hα emission line.

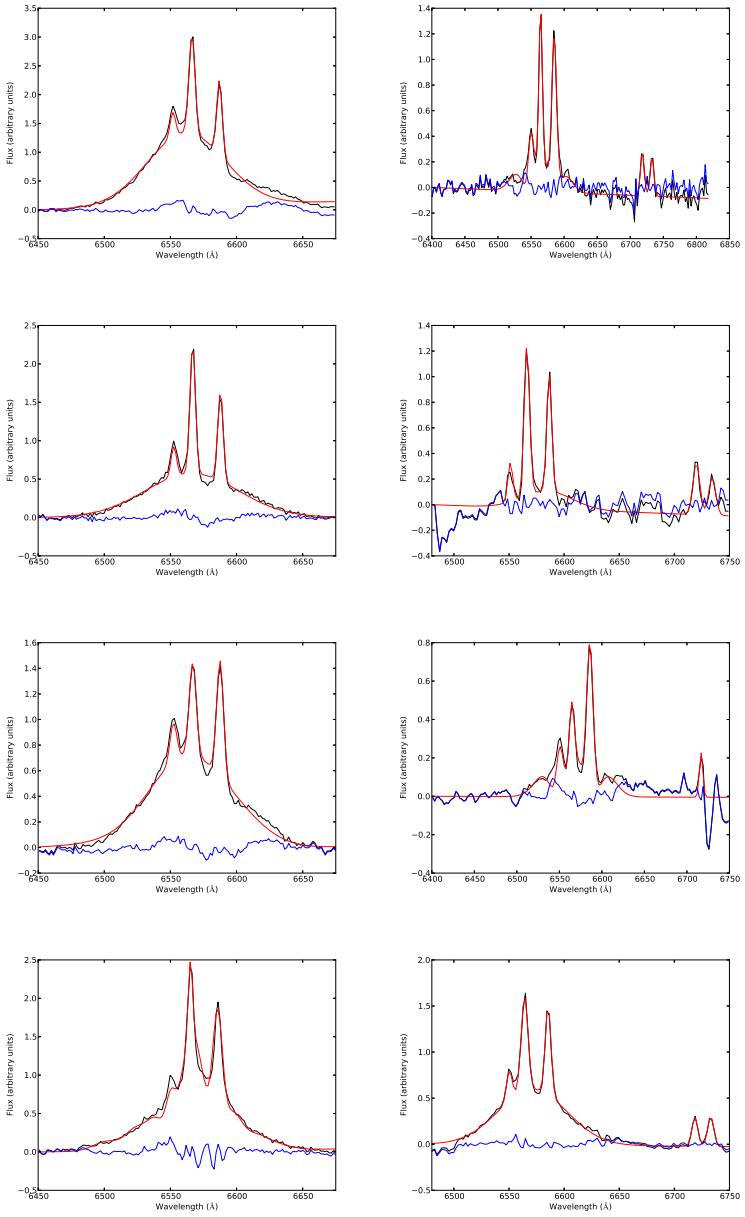

Figure 13: Same as in Figure 12 for objects 8, 27, 28, and 157.

In figures 12 and 13, objects 40, 207, 8, and 27 show significantly reduced Hα emission in Lick spectra as compared to earlier Sloan spectra. While we lack spectra from Keck in Hα for the middle of observations, and thus can not draw any conclusions

about the behavior of Hα over the time intermediate between Lick observations and SDSS, the apparent lack of strong broad Hα in Lick spectra is suggestive of time variability between Sloan observations and Lick observations.

4.4 Seyfert Type Classification

The variability of the emission lines suggests changes in classification of these objects from Type 1 AGN to Type 1.5, 1.8 or 1.9 AGN (defined in § 1.4). New classifications for each object are made on the basis of the strength of the Hα and Hβ emission line in Keck and Lick spectra. Table 3 gives the initial classification in Sloan, the classification based on Lick spectra and the dates of observation.

Object #	Sloan Classification	2009-2013 Classification
8	Type 1	Type 1.8
27	Type 1.5	Type 1.9
28	Type 1	Type 1.8
157	Type 1	Type 1.9
209	Type 1.5	Type 1.9
207	Type 1.5	Type 2
38	Type 1.8	Type 1.9
40	Type 1.5	Type 1.9

Table 3: Classification of the eight objects from SDSS and Keck/Lick spectra based on emission line profiles.

Object 8 shows pronounced broad Hβ and Hα lines in SDSS spectra, while having weak broad Hβ and visible Hα in Keck, leading to classification of a type 1 AGN in SDSS and type 1.8 in Keck. Object 27 has identifiable broad Hβ and strong broad Hα in SDSS, and no identifiable Hβ in Keck, leading to classification as a type 1.9 in Keck and type 1.5 in SDSS. Object 28 has spectral features typical of a type 1 Seyfert in SDSS and type 1.9 in Keck. Object 157, as well, has a characteristically broad component in Hβ in SDSS, and broad Hα lines, typical of a type 1 Seyfert, while missing any identifiable Hβ in Keck and retaining visible Hα, suggestive of a type 1.9. Object 209 has an identifiable Hβ broad component in SDSS, typical of a type 1.5, while lacking this feature and showing weak Hα in Keck, more typical of a type 1.9. Object 207 is similarly 1.5 in SDSS, and lacks broad lines in Keck in both Hβ and Hα, indicative of a type 2 Seyfert. Object 38 has an identifiable, but weak Hβ broad component in SDSS, typical of a type 1.8. This is weaker in Keck, more typical of a type 1.9. Finally, object 40 has identifiable Hβ in SDSS, but none in Keck, indicative of a type 1.9.

4.5 Effect of Seeing and Telescope Non-Centering

A concern in assessing the possibility of time variability of the broad emission lines is the telescope pointing. If the telescopes were not centered on the AGN during observations this could result in the presence of narrow lines, which occur over larger distance scales, and would be more difficult to miss, while not showing the broad line region. In order to test this scenario for the Keck data, flux variation in broad emission on the nights observations were taken were compared to how flux from standard stars on those nights varied. Figure 14 is an example column plot for spectra taken from a standard star.

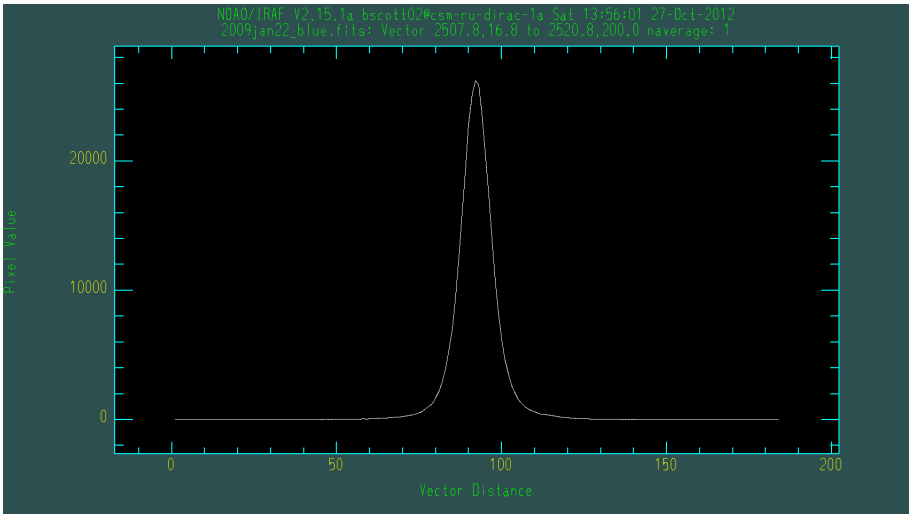

Figure 14: Example standard star PSF for the night of January 22, 2009. The PSF measures how light from a point source is scattered by the atmosphere. The x axis is pixels and the y axis is flux per pixel.

The distinctive Gaussian profile of the standard star flux profile is due to the effects of seeing. Seeing refers to the impact of turbulence in the atmosphere that causes blurring of astronomical images This causes a point like source to be spread out, and a corresponding point spread function (PSF) results. Figure 11 represents the PSF for a standard star, providing a measurement of flux as a function of pixels on the CCD camera.

In order to estimate the degree to which the telescope would have to have been offset from the AGN nucleus, the narrow to broad Hβ integrated flux ratio was examined. For Sloan spectra, the integrated flux ratios were computed using a python script written by Matthew Auger. For Keck spectra, the script was modified by Vardha N. Bennert to compute the integrated flux remaining in the residuals if a broad component is excluded by the fit. The idea is to consider the maximum possible flux in broad Hβ emission underlying the fit.

This provides an estimate of the total possible flux over a fit region in Hβ. The ratios are compared the spatial variation of a standard star for each night. The flux

from the standard star falls off as a function of pixel on the CCD, and allowed for a conversion between flux and distance, i.e. by determining the point at which a given percentage of the standard star flux occurs as a function of pixel size, one can estimate the offset required to observe the flux given by the integration of any possible broad emission. This procedure was carried out and the results are summarized in table 4.

Object #	Seeing (Pixels) (arcsec)	Broad Hβ Flux (as % of SDSS)	Distance (Pixels)	Distance (arcsec)
8	8 (1)	4	15	2
27	9 (1.2)	1	>12.5	>1.7
28	9 (1.2)	5	12.5	1.7
157	9 (1.2)	5	12.5	1.7
209	6 (0.8)	3	9	1.2
207	6 (0.8)	2	9	1.2
38	7 (0.9)	7	10	1.3
40	7 (0.9)	11	10	1.3

Table 4: Estimated broad emission line flux for Keck as a percentage of flux in SDSS. This value is translated using the fall off in flux as a function of pixel size recorded for a standard star, and converted to arcseconds using a conversion specific to the instrument. This value is compared to the seeing in pixels.

Based on the seeing, we do not believe that the telescope was likely to have been offset from the host galaxy nucleus to the degree necessary to account for the variation. The offset required to account for the reduction in broad line flux is approximately 1.5-2 times the seeing on each night, with a seeing of 0.8-1.2 arcsec and typical pointing accuracy of the Keck telescope, it is unlikely that such a large offset is responsible for the change in broad line flux.

5 Discussion

In order to account for the lack of clear broad Hβ lines in Keck and Lick spectra as compared to the previous SDSS spectra, as well as the lack of Hα in Lick as compared to SDSS, we now consider a series of potential explanations. It is important to note, first, that each explanation may only account for a subset of our sample, and second, that not all explanations are testable with data currently available. The explanations we consider are, (i) a supernova occurring in the host galaxy during Sloan observations which decays over time, (ii) variation of the BLR or the torus, and (iii) non-coincident BLR, for example, due to gravitational recoil of the SMBH or an ongoing merger.

5.1 Supernova

A possible scenario explaining the presence of broad emission lines in SDSS spectra as opposed to later Keck and Lick spectra is a supernova event in the host galaxy prior

to Sloan observations but which was no longer visible by the time of Keck and Lick observations. Under this scenario, the galaxy does not host an AGN, but instead the spectra are of a supernova in the central regions of the host galaxy.

Spectra from supernova can appear quite similar to AGN spectra, replicating the distinct broad emission line profiles of Balmer (and other) lines which distinguish type 1 Active Galaxies [8]

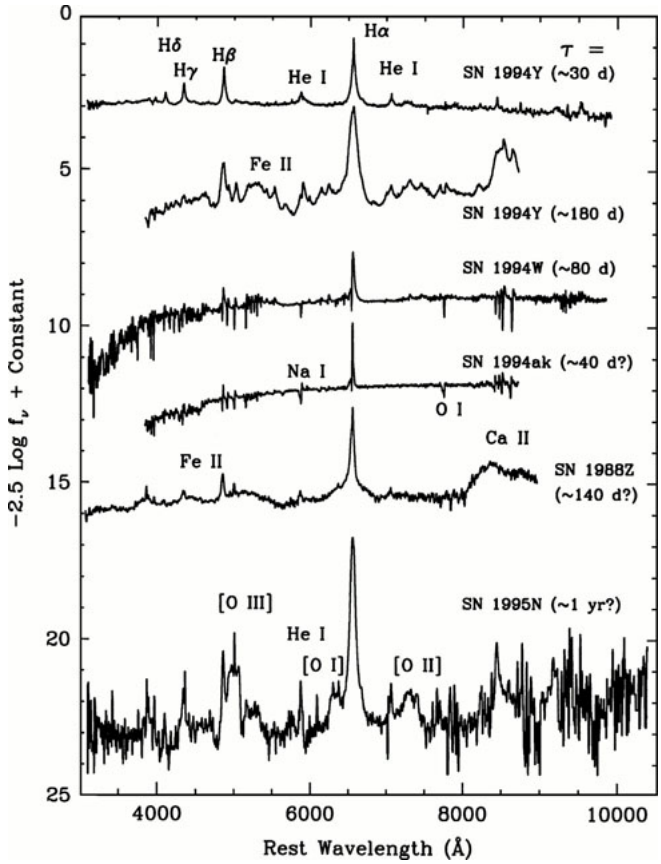

Figure 15: Several type IIn supernova spectra showing strong narrow Hα emission and a weak broad component. [8]

Type IIn supernova, a highly luminous event which occurs when a very massive star collapses and explodes at the end of its life, preferentially show hydrogen emission lines in spectra. These are believed to result from the interaction of Supernova ejecta with a dense circumstellar medium and are also associated with strong X-ray emission (Komossa, 2009 and references therein). These events could produce the appearance of both broad and narrow emission lines typical of type 1 AGN in earlier spectra. A potential scenario is therefore suggested. Assuming that broad Hβ emission fades prior to broad Hα emission, SDSS would show a typical Type 1 AGN spectra, while Keck and Lick would show a spectra in Hβ typical of a Type 1.5, 1.8 or 1.9 AGN. Since

Hα is observed in some Lick spectra, broad Hβ emission must fade faster (e.g. due to changing dust obscuration) for this scenario to fit the observations.

Type IIn supernova are characterized, as their name suggests, by a very strong narrow emission line component superimposed upon a weaker but extended broad emission line component. Figure 15 is a collection of type IIn supernova spectra. In these objects, Hα emission is typically stronger, and in some cases, there is considerable variability in the line profile of Hα on comparatively short time scales (days to years), with periods of strong and weak broad Hα emission. In other cases, supernova have considerable variability in the narrow emission lines produced by forbidden transitions. Interestingly, the broad Hα component has been observed to be offset from the velocity of the parent galaxy, which may be similar to features expected of recoiling SMBH (§ 5.3.2). Fe II, Ca II, O I, and Na I absorption is associated with supernova of this type, as well, especially at early times. [8]

The considerable variability between individual Type IIn supernova complicates distinguishing between supernova and AGN spectra, however, the AGN line ratios are typically not met by supernova, and the narrow Hα component is typically much stronger than the broad component for supernova. Despite this, supernova remain a likely explanation for the observed time variability of the Hα and Hβ emission lines in the sample.

5.2 Variation of the Continuum Source, Broad Line Region or the Torus

One possibility is that the BLR itself varies in some way, which produces a reduction in flux in the broad lines. The BLR consists of hydrogen emission clouds orbiting the central engine. These emission clouds are not uniformly dense, and it is therefore possible that the observed emission line profiles will vary according to changes in the apparent "clumpiness" of the BLR itself.

A recent study of the AGN in 3C 390.3, NGC 4151, and NGC 5548, observed over a period of 10 years, showed transitions between Type 1 and Type 1.8. The authors concluded that the transition could be explained by a BLR close to the central engine, and is associated with changes in the accretion disk and the continuum. [9]

Another study reports the reverse process - the appearance of broad Balmer lines in previously observed objects lacking those lines. [10] They concluded similarly on the basis of asymmetries in line profiles, that the appearance of these lines is due to changes in the accretion disk resulting from a stellar disruption event, an event which occurs when a star ventures too near the black hole and is disrupted by tidal forces. This process results in material from the star accreting onto the black hole which leads to changes in continuum emission.

An alternative explanation is variation of the dusty torus, which surrounds the broad line region. A study connected the appearance of broad lines in Type 2 AGN to a change in the reddening of the dusty torus. [11] This transition may also have been associated with changes in the continuum. The authors of this study report that X-ray observations are required to examine this hypothesis in more detail.

A scenario is suggested: SDSS observes the AGN early in the decade while changes in the BLR region or the torus lead to the apparent disappearance of broad emis-

sion lines in our spectra taken 10 years later and remain absent in follow-up Lick Spectroscopy. These objects, therefore, underwent a transitory event (reddening of the torus or continuum change etc.) coinciding with SDSS observation, appeared to be type 1, leading to their inclusion in our survey, and have now returned to their intrinsic type 2 classification.

5.3 Offset SMBH and Emission Line Regions

In considering mechanisms, we have tacitly assumed that the AGN, meaning the black hole, accretion disk and the broad line region were coincident with the center of their host galaxy. It is also possible that the BLR is not coincident with the luminous bulge of the galaxy which has been the centering target for the telescope in each survey. The challenge for this explanation is understanding why SDSS, which also centered on the approximate center of the host galaxy, detected broad emission, while Keck and Lick did not.

While the process which would give rise to a noncoincident BLR is, itself, somewhat ambiguous and may be different in each case, the first columns of figure 10 and 11 explain how the broad line region would be captured by SDSS observations, while not being captured by Keck or Lick. The 3" fiber of the Sloan Survey captures a circular region surrounding the central regions of the host galaxy, while the Keck and Lick slits are only capable of observing the swath indicated in figure 11. If the BLR lies within the 3" fiber, but outside of the slit, it would appear in SDSS, but not in Lick or Keck. However, the appearance of broad Hα in each Lick spectra would appear to discount this possibility for those objects which had the same slit orientation between Keck and Lick (see figures 10 & 11, § 4.3.1).

5.3.1 Ongoing Merger

An ongoing merger could produce an offset AGN source if the primary (i.e. larger) galaxy were inactive and the secondary (i.e. smaller) galaxy were active. This would produce the appearance of an AGN offset from its host galaxy, as in figure 16.

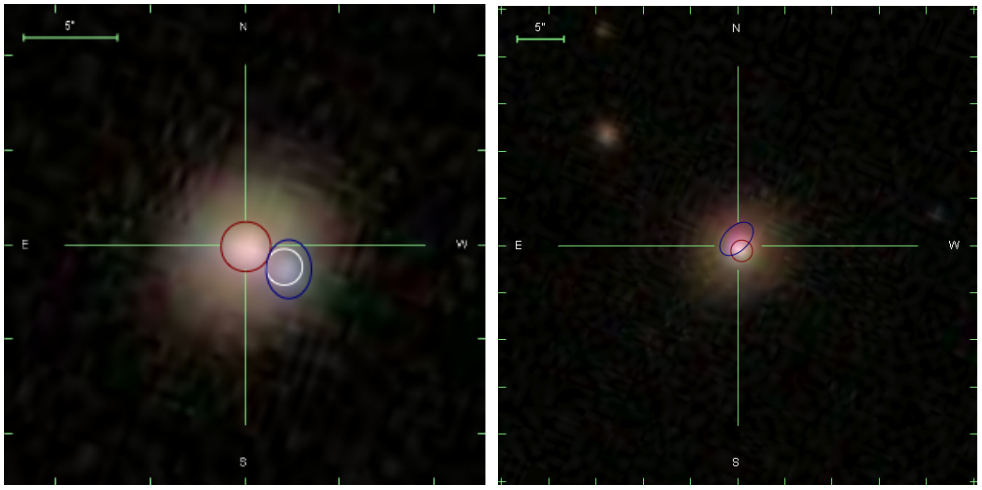

Figure 16: SDSS images of objects 157(left) and 8(right) showing both a central luminous region(red), which is the centering target for each observation and knot like structures offset from this region. The knot structure for 157 is highlighted in white, with blue indicating the furthest extent of such a structure, and is highlighted in blue for object 8.

Object 157 has a clear knot in SDSS optical image. As noted by William Keel during data reduction, the peak of the narrow emission lines is offset 1.5" from the luminous bulge of the host galaxy. This offset is consistent with the location of the knot in the SDSS image, and suggestive of an offset AGN source.

There are two observational signatures of an ongoing merger that place constraints on this scenario. The first is signs of tidal disruption in optical images, as the secondary galaxy merges with the primary, Tidal tails should form if the merger is "large", what is typically termed a "major merger". Major mergers are mergers that occur between two galaxies of comparable mass. A smaller scale merger, i.e. between a galaxy with a larger mass compared to a smaller mass secondary (e.g. by a factor of 1/3) can occur without these tidal features remaining visible in the shallow SDSS images. The second constraint is that mergers, even minor mergers, are believed to be able to trigger AGN activity. [12] This occurs in the case that both progenitor galaxies are host to an SMBH, a reasonable assumption but not necessarily true of all galaxies.

Under an ongoing merger scenario, it is expected that galaxy will enter a dual AGN phase, while the SMBH of the primary and secondary galaxies both enter an active phase. This dual AGN scenario is characterized by double peaked narrow [O III] lines, which are not present in our spectra. [13]

Another constraint comes from the timescales of mergers compared to the onset of AGN activity. If the time scale for relaxation of the tidal tails is shorter than the onset time of AGN activity following a merger, than the lack of tidal tails places no constraint on the likelihood of this scenario. Alternatively, if the time scale of AGN activity is much less than the relaxation time of the tidal features, than this scenario is severely constrained by the presence or lack of these structures.

5.3.2 Recoiling Supermassive Black Hole Candidates?

Among possible explanations for the noncoincidence of the SMBH and BLR with the center of the host galaxy is that the central black hole could be undergoing gravitational recoil following a merger of two progenitor BHs.

Gravitational recoil occurs when linear momentum is carried away by the anisotropic emission of gravitational radiation following the merger of black holes. [14]. This process causes the center of mass of the system to recoil. [15] Taking into consideration the spin of the merging black holes, the "kick velocities" attained by black holes are in the hundreds, or thousands, of km/s [16]. These velocities are larger than the escape velocity of some small galaxies, allowing the possibility of SMBH which have been or are in the process of being ejected from their host galaxy.

If a black hole is not ejected from its host galaxy, the black hole will oscillate on long time scales. In the majority of cases, however, the black hole will instead oscillate around the nucleus. This is caused by dynamical friction, the combined effect of gravitational interactions between the black hole and material in the host galaxy, and the initial kick due to recoil. The result is that the black hole will exhibit damped oscillatory motion about the central regions of the galaxy. The decay of this oscillation will occur on timescales of up to $\approx$ 1 Gyr, and the oscillations will occur on spatial scales as large as the size of the bulge. [17] In other words, the central SMBH can be observed outside the center and as far offset as the egde of the bulge with reasonably high probability.

As the black hole recoils away from the central regions, regardless of whether it is ejected completely from the host galaxy or oscillates about the central regions, it may drag the BLR and accretion disk with it since these are gravitationally bound to the SMBH. [14] Since the NLR region is not in the potential of the AGN, the BLR will have a different velocity, and hence redshift or blueshift, than the NLR if there is a component of its velocity which is perpendicular to our line of sight. The result is that the BLR will be offset from the NLR with an apparent asymmetry in the broad emission line profile. This asymmetry arises from the velocity offset due to the motion of the recoil along a direction parallel to an observers line of sight. The line becomes offset from the narrow component.

There are two candidates for this process in the sample. Objects 8 and 157 both have visible "blobs" or "knots" in optical images (see figures 10 and 11). It was initially assumed that the blob may be an SDSS artifact due, for example, to a mismatch in the image registration of the five filters that produce the colored image. However, instead it may be the BLR, accretion disk and SMBH undergoing recoil. In both cases, the AGN is approximately one bulge radius offset from the center, consistent with theoretical constraints, and may have been captured by the SDSS fiber, while possibly remaining outside the Keck 1 arcsec slit. Also, there is some asymmetry in the Hβ emission line, consistent with the recoil mechanism.

The Lick slit was placed such that it would lie across the central regions of object 157 and the "blob"/companion in order to confirm or rule out this scenario. While the Lick spectra show continued broad Hα emission, there remains significantly reduced broad Hβ, making this scenario unlikely. While the slit was not placed with the intention of taking spectra of a possible offset AGN, object 8, similarly, shows a continued lack of

broad emission in Hβ in Lick spectra, and the slit was oriented such that light from a possible offset BLR should scatter into the slit given the seeing conditions.

Variability of X-ray emission is associated with recoil behavior, and object 157 has been identified as an X-ray source with observations from the space based Chandra X-ray observatory available. [18] Analysis of these observations is ongoing (§ 6).

While object 8 and object 157 remain candidates for recoiling AGN, the likelihood of this scenario is comparatively low. High resolution images and spectroscopy are necessary to probe this scenario in more detail. In both cases, the key observational test of this scenario would be to observe offset broad emission from the knots. This is complicated by competing effects. If the recoil velocity is large parallel to an observers line of sight, the broad emission lines will have strong kinematic offsets. Simultaneously, the spatial offset corresponding to the kinematic offset will be small, since spatial offsets will be observed perpendicular to the line of sight. Of course, this argument is symmetric. The small kinematic offset and large spatial offset in L157 are expected if the velocity of the recoiling SMBH is directed perpendicular to our line of sight. The small kinematic offset and large spatial offset in L157 is consistent with this possibility. Further, the time scale arguments of the previous section (§ 5.3.1) place further constraints on this scenario.

6 Conclusions & Outlook

This paper has identified eight instances of local Seyfert galaxies exhibiting signs of emission line variability in Hα and Hβ. Constraints on time scale are made, and based on seeing and PSF profile arguments, we can exclude that the lack of broad lines in the Keck spectra are caused by the telescope being pointed off center, missing the active nucleus. In follow-up spectra taken at Lick Observatory, the broad emission lines remain missing in Hβ and are missing or reduced in Hα, suggesting changes in Seyfert classification transitions on timescales of approximately a decade. Despite not being able to conclude definitively in favor of any explanation for this variability, observational constraints make changes in the torus or broad-line region over time as the most likely cause for this variation. However, at least in some cases, the existence of an AGN that is non-coincident with the center of the host galaxy due to an ongoing merger or gravitational recoil cannot be ruled out. The most promising candidate for such a scenario is object 157, which shows a blue knot just off-center from the host galaxy, and has offset AGN emission associated with this location.

The outlook for our study of time variability in local AGN is good, however. The next steps in our analysis will be quantify the change in Hα emission between Lick and SDSS, in a manner similar to that conducted for Hβ (§ 4.5), to look for signs of continuum emission which may be associated with broad line variability and to probe X-ray and radio observations for these galaxies. While we can exclude the complete loss of the broad lines due to noise in Keck and Lick spectra, we hope to quantify the impact of noise on the disappearance of weak extended broad features.

While further observations in a wide portion of the spectrum are required to pin down the mechanism underlying this process, the large size of the sample, approximately 100 objects, allows for statistics to be gathered on the frequency of changes in

Seyfert type transitions, with approximately 8-9% of AGN exhibiting this time scale variability over a time frame of a decade or less. The mechanism underlying these changes may also be different across the objects undergoing transitions, and may also be a combination of each mechanism discussed. Further, the variability of the broad Hβ emission line may make it a poor candidate for measurement of the mass of the central engine from single-epoch spectra, at least for those objects which are prone to undergoing these transitions.

Our discussion of the various scenarios, variability of the torus or BLR, supernova, or noncoincident AGN is unable to conclude in favor of any of the potential explanations.

As is typical of the scientific process, more observations are necessary to draw any further conclusions.

7 Acknowledgements

I would like to acknowledge the support of Vardha N. Bennert, who has helped me to mature as a scientist and as a student while completing this project. I would also like to acknowledge the contributions of Matthew Auger, who wrote the python scripts used to conduct fitting, and William Keel for reducing the Lick data. I would like to thank Anna Pancoast for her assistance in conducting observations at Lick Observatory, and Stefanie Komossa for her input on possible mechanisms, including supernova and SMBH recoil.

References

[1] B.M. Peterson, *An Introduction to Active Galactic Nuclei.* (Cambridge University Press, Cambridge, UK 2003), pp. 21-109.

[2] L. Ferrarese, H. Ford, Supermassive Black Holes in Galactic Nuclei: Past, Present and Future Research. Space Science Reviews. February 2005, Volume 116, Issue 3-4, pp 523-624.

[3] D.E. Osterbrock, Astrophysics of Gaseous Nebulae and Active Galactic Nuclei. (University Science Books, Mill Valley, CA.) 1989.

[4] V.N. Bennert, M.W. Auger, T. Treu, J. Woo. M. Malkan, A Local Baseline of the Black Hole Mass Scaling Relations for Active Galaxies. I. Methodology and Results of a Pilot Study. The Astrophysical Journal, January 2011, Volume 726, Issue 2.

[5] C.E. Harris, V.N. Bennert, M.W. Auger, T. Treu, J. Woo. +1, A Local Baseline of the Black Hole Mass Scaling Relations for Active Galaxies. II. Measuring Stellar Velocity Dispersion in Active Galaxies. The Astrophysical Journal Supplement, August 2012, Volume 201, Issue 2.

[6] K. Gultekin, D.O. Richstone, K. Gebhardt, T.R. Lauer, S. Tremaine, The M-σ and M-L Relations in Galactic Bulges, and Determinations of their Intrinsic Scatter. The Astrophysical Journal, June 2009, Volume 698, Issue 1.

[7] M. Volonteri, The Formation and Evolution of Massive Black Holes. Science. August 2012, Volume 337, no. 6094.

[8] A.V. Filippenko, Optical Spectra of Supernova. Annu. Rev. Astron. Astrophys. 1997.35:309-355.

[9] A.I. Shapovalova, L.C. Popovic, N.G. Bochkarev, A.N. Burenkov, V.H. Chavushyan, Long Term Variability of the Broad Emission Line Profiles in AGN. arXiv:astro-ph/0908.2763v2. September 2009.

[10] M. Eracleous, J.P. Halpern, NGC 3065: A Certified LINER with Broad, Variable Balmer Lines. The Astrophysical Journal. Preprint arXiv:astro-ph/0101050v1. January 2001.

[11] I. Aretxaga, B. Joguet, D. Kunth, J. Melnick, and R.J. Terlevich. Seyfert 1 Mutation of the Classical Seyfert 2 Nucleus NGC 7582. The Astrophysical Journal. Volume 519, Issue 2. July 1999.

[12] A.R. Draper and D.R. Ballantyne. A Tale of Two Populations: The Contribution of Merger and Secular Processes to the Evolution of Active Galactic Nuclei. The Astrophysical Journal. Volume 751, Issue 1. May 2012.

[13] Comerford, J. Observations of Dual Supermassive Black Holes at kpc-scale Separations. Massive Black Holes: Birth, Growth and Impact. Kavli Institute for Theoretical Physics. August 2013. Unpublished Conference Proceedings.

[14] S. Komossa, H. Zhou, and H. Lu. A Recoiling Supermassive Black Hole in the Quasar SDSS J092712.65+294344.0. The Astrophysical Journal. Volume 678, Issue 2. May 2008.

[15] A. Peres. Classical Radiation Recoil. Physical Review. Volume 128, issue 5. December 1962.

[16] M. Campanelli et. al. Larger Merger Recoil and Spin Flips from Generic Black Hole Binaries. The Astrophysical Journal. Volume 659, Issue 1. 2007.

[17] A. Gualandris and D. Merritt. Ejection of Supermassive Black Holes from Galaxy Cores. The Astrophysical Journal. Volume 678, Issue 2. 2008.

[18] S. Komossa. Recoiling Black Holes: Electromagnetic Signatures, Candidates, and Astrophysical Implications. Advances in Astronomy. Volume 2012. id. 364973.